Double-resonant x-ray and microwave absorption:
Atomic spectroscopy of precessional orbital and spin dynamics

G. Boero,[1] S. Rusponi,[1] P. Bencok,[2] R. Meckenstock,[3] J.-U. Thiele,[4] F. Nolting,[5] and P. Gambardella[6,7,*]

[1]*Ecole Polytechnique Fédérale de Lausanne (EPFL), CH-1015 Lausanne, Switzerland*
[2]*European Synchrotron Radiation Facility (ESRF), F-38043 Grenoble, France*
[3]*Fachbereich Physik, Universität Duisburg-Essen, D-47048 Duisburg, Germany*
[4]*Hitachi Global Storage Technologies, San Jose Research Center, San Jose, California 95135, USA*
[5]*Swiss Light Source (SLS), Paul Scherrer Institut, CH-5232 Villigen PSI, Switzerland*
[6]*Institució Catalana de Recerca i Estudis Avançats (ICREA), E-08100 Barcelona, Spain*
[7]*Centre d'Investigació en Nanociència i Nanotecnologia (ICN-CSIC), UAB Campus, E-08193 Bellaterra, Spain*

We show that double-resonance spectra recorded during the simultaneous absorption of x-ray and microwave (MW) photons are a fingerprint of the perturbed electronic configuration of atomic species driven to ferromagnetic resonance. X-ray absorption measurements performed as a function of x-ray energy and polarization over the Fe $L_{2,3}$ edges of single-crystal yttrium-iron garnet reveal MW-induced multiplet features related to angular momentum transfer from the MW field to localized Fe $3d$ magnetic sublevels. O K-edge absorption spectra demonstrate the formation of dynamic $2p$-orbital magnetization components at O sites coupled to the Fe magnetic moments at tetrahedral and octahedral sites. These results are compared with double-resonance x-ray absorption spectra of Permalloy, showing that the MW transition probability is distributed according to the hybridization character of the $3d$ states and proportional to the unperturbed unoccupied magnetic density of states of metals and insulators.

I. INTRODUCTION

Double-resonance spectroscopy techniques based on the simultaneous absorption of optical and microwave (MW) photons have a long history in the study of magnetic resonance.[1–5] Both the excited- and ground-state electronic structures of paramagnetic atoms can be determined by detecting the absorption or emission of light modulated by a MW field, which may also serve to distinguish ions or molecules with different optical-absorption lines and measure spin-lattice relaxation times.[6,7] The analogous approach to detect ferromagnetic resonance (FMR) relies on the MW modulation of the Faraday[8] and Kerr[9] effects. In ferromagnets, however, broad optical-absorption bands and exchange coupling concur to conceal local electronic structure effects, restricting these techniques to the observation of collective magnetization modes and precession angles, similarly to inductive methods. By replacing visible light with polarized x-ray photons from a tunable synchrotron source, significant new insight can be obtained due to the inherent localization of core-level x-ray absorption processes. Information about the electronic ground state, including the occupation and mixing of the valence electronic levels, crystal field, spin orbit, and exchange interactions is encoded in the energy-dependent spectral line shape as a function of photon energy, and can be extracted through multiplet calculations and sum rules.[10]

Recently, several efforts have been made to combine the element sensitivity of x-ray absorption with magnetic-resonance measurements using either time-resolved[11–15] or time-invariant[16–21] schemes. Such experiments, carried out at fixed x-ray energy, enabled the measuring of element-resolved FMR spectra of pure and rare-earth-doped yttrium-iron-garnet (YIG),[16–21] metal films,[17] as well as the relative phase and precession angle of the magnetization in coupled metal layers.[13,14] Here, we report on the first measurements of x-ray absorption spectra recorded simultaneously with continuous-wave resonant MW excitations as a function of x-ray photon energy and polarization. We demonstrate that double-resonance x-ray absorption spectroscopy (XAS) is a probe of the localized electronic excitations induced by MW transitions that give origin to FMR, including the absorption of angular momentum from MW photons to valence electrons and related formation of site-specific precessing magnetic moments. Circularly and linearly polarized double-resonance $L_{2,3}$ x-ray absorption spectra of Fe in a single-crystal YIG provide clear evidence of the transfer of angular momentum from the MW field to Fe^{3+} $3d$ magnetic sublevels, leading to the precession of octahedral (O_h) and tetrahedral (T_d) Fe^{3+} species. Double-resonance O K-edge spectra reveal that O sites are dynamically active with angular momentum being transferred to states with mixed $2p$-$3d$ character and inducing the formation of precessing orbital-moment components coupled to the Fe magnetization. We compare double-resonance Fe spectra of YIG and Gd-doped Permalloy, showing that the spectral line shape depends on the localized versus metallic character of the MW-perturbed states. The energy-dependent line shape of the double-resonance x-ray magnetic circular dichroism (XMCD) signal is generally found to mirror the static XMCD intensity, showing that the probability of MW absorption in either a magnetic insulator or a metal is homogeneous over the states sampled by x-ray absorption and proportional to the unoccupied magnetic density of states (DOS).

Double-resonance measurements offer an alternative to broadband time-resolved x-ray absorption experiments,[22,23]
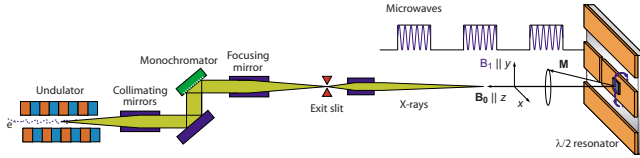
FIG. 1. (Color online) Schematic diagram of the experiment.

allowing for selecting the frequency of the electromagnetic excitations and combining two powerful spectroscopic tools into one. Without requiring flux-limited synchrotron operation modes, dual-resonance schemes involving time-invariant magnetic-resonance detection provide a comparatively short measuring time and excellent signal-to-noise ratio, and may be adapted to study both ferromagnetic- and paramagnetic-resonance phenomena in a very broad frequency range.

This paper is organized as follows: Sec. II describes the experimental method. The x-ray absorption spectra of resonantly excited YIG and Permalloy are reported and discussed in Sec. III A and Sec. III B, respectively, side-to-side with conventional x-ray absorption spectroscopy results. XMCD spectra are compared in Sec. III C. In the Appendix, we discuss the origin of the MW-induced multiplet features and introduce a general model for interpreting double-resonance measurements in the x-ray regime, which is shown to apply for different materials and absorption edges.

II. EXPERIMENTAL METHOD

Figure 1 shows a schematic diagram of the dual-resonance experimental setup. The experiments were performed at the surface/interface microscopy beam line of the Swiss Light Source using tunable 0.5–1 keV synchrotron radiation with $99 \pm 1\%$ polarization rate generated by two helical undulators operated in series. FMR was excited by a 2.25 GHz MW field $\mathbf{B}_1$ generated by a coplanar waveguide $\lambda/2$ resonator oriented perpendicularly to the x-ray incidence direction $\hat{\mathbf{z}}$. The samples were placed on top of the resonator and inserted into an evacuated vessel between the expansion poles of an electromagnet used to produce a sweep field $\mathbf{B}_0$ of amplitude of 0–0.8 T aligned parallel to the x-ray beam and perpendicular to $\mathbf{B}_1$, as described in Ref. 16. The input MW power from a tunable MW source was set to 35 dBm, corresponding to $B_1 \approx 0.5$ mT. Excitation frequencies up to 10 GHz were successfully tested using different sets of resonators. The monochromatic x-ray beam was focused to a 100×100 $\mu\mathrm{m}^2$ spot and constantly illuminated the sample. By tuning the x-ray photon energy to the $2p \rightarrow 3d$ ($1s \rightarrow 2p$) thresholds of Fe (O) and adjusting $\mathbf{B}_0$ to induce FMR at the chosen MW frequency, a double-resonance experiment was realized, where core-level excitations probe MW absorption taking place in the valence shell. The XAS intensity was measured in the fluorescence-yield (FY) mode for circularly positive (I^+), negative (I^-), and linearly $x-$, $y-$($I^{x,y}$) polarized light at the $L_{2,3}$ ($2p \rightarrow 3d$) edges of Fe and K ($1s \rightarrow 2p$) edge of O. To detect MW-induced changes in the XAS signal, the MW source was pulse modulated at a frequency of 3.4 kHz with 50% duty cycle. The FY photocur-

rent was split into dc-(I_{dc}) and ac-amplified signals, and the latter fed into a lock-in amplifier set to measure the amplitude of the input signal at the pulse-modulation frequency (I_{ac}). The ac photocurrent represents the double-resonance x-ray absorption intensity. Both dc and ac XAS spectra were normalized to the incident photon flux using the electron-yield signal from the first mirror upstream from the sample. Apart from flux normalization, dc and ac data are presented as measured; in particular, no correction for self-absorption FY effects has been applied. Unless otherwise specified, (I_{ac}) units are given as fraction of the (I_{dc}) intensity. Measurements were taken on a 7-μm-thick, 1×4 mm^2 single-crystal YIG film grown by liquid epitaxy on gadolinium-gallium garnet, and a polycrystalline Ta(5 nm)/ $Ni_{72}Fe_{18}Gd_{10}$(30 nm)/Ta(1 nm) layer grown by dc-magnetron sputtering on glass. Gd doping of Permalloy was introduced to reduce the film saturation magnetization because of Gd-Ni and Gd-Fe antiferromagnetic couplings, thus decreasing the resonance field of $Ni_{72}Fe_{18}Gd_{10}$ within the range of $\mathbf{B}_0$.

III. RESULTS

A. Double-resonant x-ray microwave absorption in YIG

Figure 2 (left column) shows the dc XAS of Fe measured at the $L_{2,3}$ edges with the corresponding XMCD typical of the ferrimagnetic alignment of O_h and T_d Fe^{3+} sites in YIG.[16,24] A central result of this work are the unusual and finely structured spectra obtained by simultaneous acquisition of the MW-induced signal I^+_{ac} and I^-_{ac} reported in the right column. Although changes in the x-ray absorption intensity are extremely weak, the order of 1 part per 1000, FMR produces strikingly different and asymmetric spectra compared to the unperturbed $L_{2,3}$ line shape. The ac signal disappears moving $\mathbf{B}_0$ off the FMR peak position and scales with the input MW power. The comparison of Fig. 2(c) and 2(f) shows that MW-induced effects are detected also in the linearly polarized components, I^x_{ac} and I^y_{ac}, for which the equality $I^x_{ac} + I^y_{ac} = I^+_{ac} + I^-_{ac}$ is quantitatively verified, as expected from the equivalence of circular- and linear-polarization basis states. These findings demonstrate that MW absorption reflects in a nontrivial way on the Fe XAS and explain a previous controversy on the intensity of FMR peaks measured using x-ray detection at fixed photon energy.[16,20] Double-resonance XAS cannot simply be interpreted using a classical description of FMR in terms of a precessing magnetization vector with reduced projection onto the beam axis and related decrease in XMCD contrast,[16,17,19,20] in analogy with optical[8,9] and inductive FMR detection methods.[25] Rather, the simultaneous occurrence of angular momentum transfer induced by both MW and x-ray absorption must be taken into account into a local quantum-mechanical framework, as exemplified in Appendix for the case of a paramagnetic Fe^{3+} ion. In such a double-resonance model, MW-induced coupling of the magnetic Zeeman sublevels perturbs the electronic ground-state population, generating high-frequency transverse spin- and orbital-magnetization components precessing about $\mathbf{B}_0$, and modifying the polarization-dependent probability of x-ray
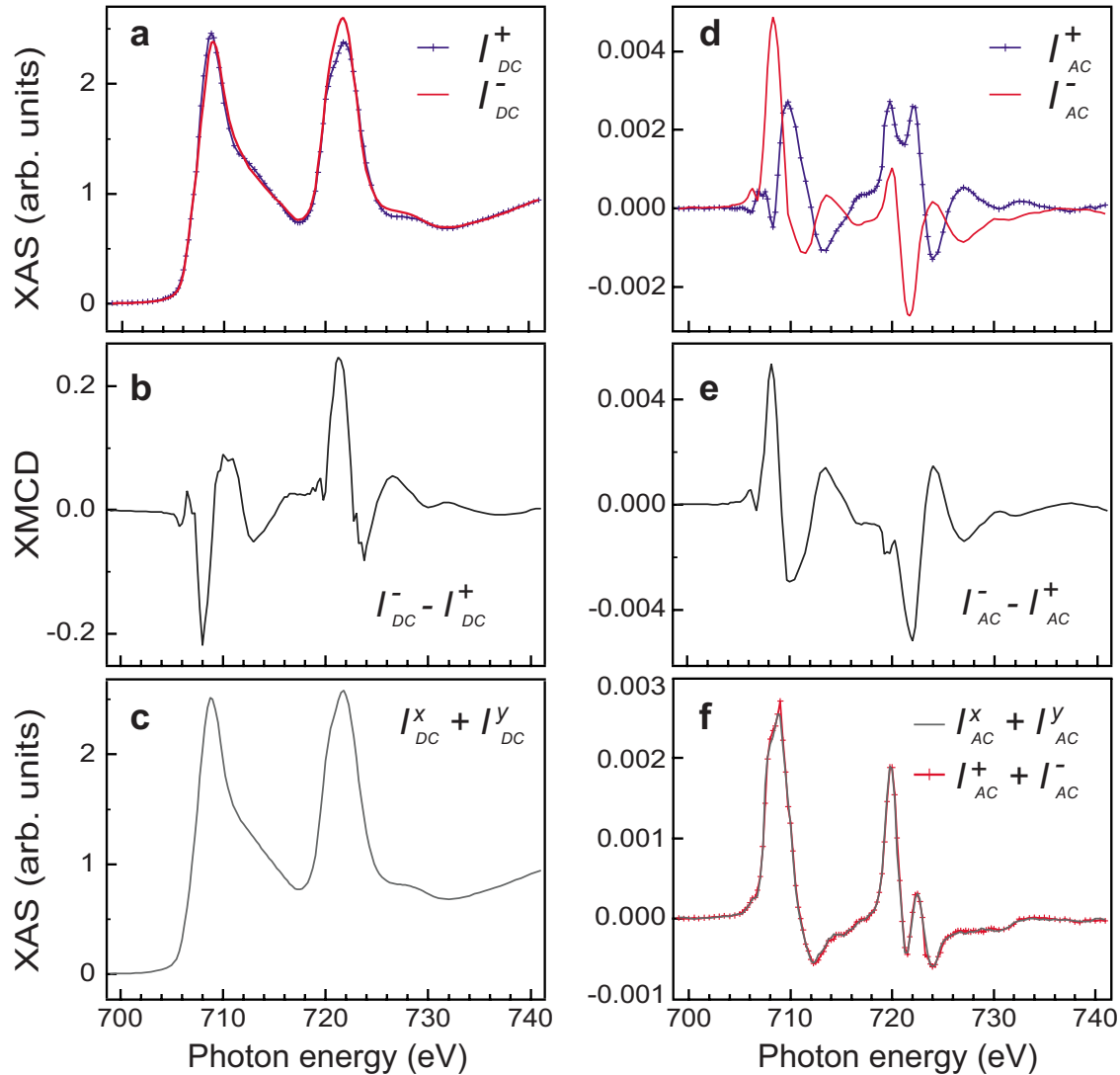
FIG. 2. (Color online) Fe $L_{2,3}$-edge absorption spectra of YIG. (a) dc fluorescence yield as a function of photon energy recorded with positive (I_{dc}^+) and negative (I_{dc}^-) circularly polarized lights. The external field is set to $B_0 = 0.205$ T to match the FMR condition. (b) dc XMCD ($I_{dc}^- - I_{dc}^+$). (c) Linearly polarized XAS ($I_{dc}^x + I_{dc}^y$). (d) Double-resonance circularly polarized spectra (I_{ac}^+, I_{ac}^-) recorded simultaneously with (a). (e) Double-resonance XMCD ($I_{ac}^- - I_{ac}^+$). (f) Comparison between the sum of double-resonance circularly ($I_{ac}^+ + I_{ac}^-$) and linearly polarized ($I_{ac}^x + I_{ac}^y$) spectral components. The dc XAS edge jump has been scaled to one; I_{ac} and XMCD units refer to the dc intensity. For each polarization, a pair of dc and ac spectra was measured in one sweep with a recording time of 1000 s.

transitions in an edge- and site-specific way. In a ferromagnet or ferrimagnet, however, this picture is significantly complicated by the presence of exchange-split-hybridized electron bands. Resonant absorption of MW occurs between spin-wave states, i.e., delocalized collective Zeeman excitations. Here, the localization of core-level transitions offers the unique ability to probe the transfer of energy and angular momentum from MW photons to specific electron orbitals, effectively projecting out a spin-wave state onto its atomic components.

As an example of this capability, we tune the x-ray photon energy to the O K edge to investigate covalency effects in ferrimagnetic oxides[26] that have scarcely been addressed by FMR studies. Despite the very small XMCD cross section of K-edge $1s \rightarrow 2p$ transitions, a weak dc XMCD signal is detected at the O edge, shown in Fig. 3. What is more remarkable in this context is that the double-resonance spectra present pronounced features due to the absorption of MW photons by O states. Contrary to Fe, I_{ac}^+ and I_{ac}^- features are symmetric and the linear $I_{ac}^{x,y}$ intensity is zero, a fact that relates to the specificity of K-edge transitions (see Appendix). The most intense MW response is found in the spectral region between 528 and 532 eV, which we associate to O states of mixed $2p$-$3d$ character arising from O-Fe hybridization.[27] In analogy with magnetite,[28] the oscillating sign of the O XMCD is attributed to O states hybridized with $3d$ orbitals of O_h and T_d Fe^{3+} atoms with antiparallel magnetic moments. As K-edge XMCD uniquely probes the p valence-shell orbital moment,[18,29] the nonzero double-resonance XMCD spectrum demonstrates the formation of precessing orbital magnetic-moment components that originate from the $2p$-projected density of states of O atoms.
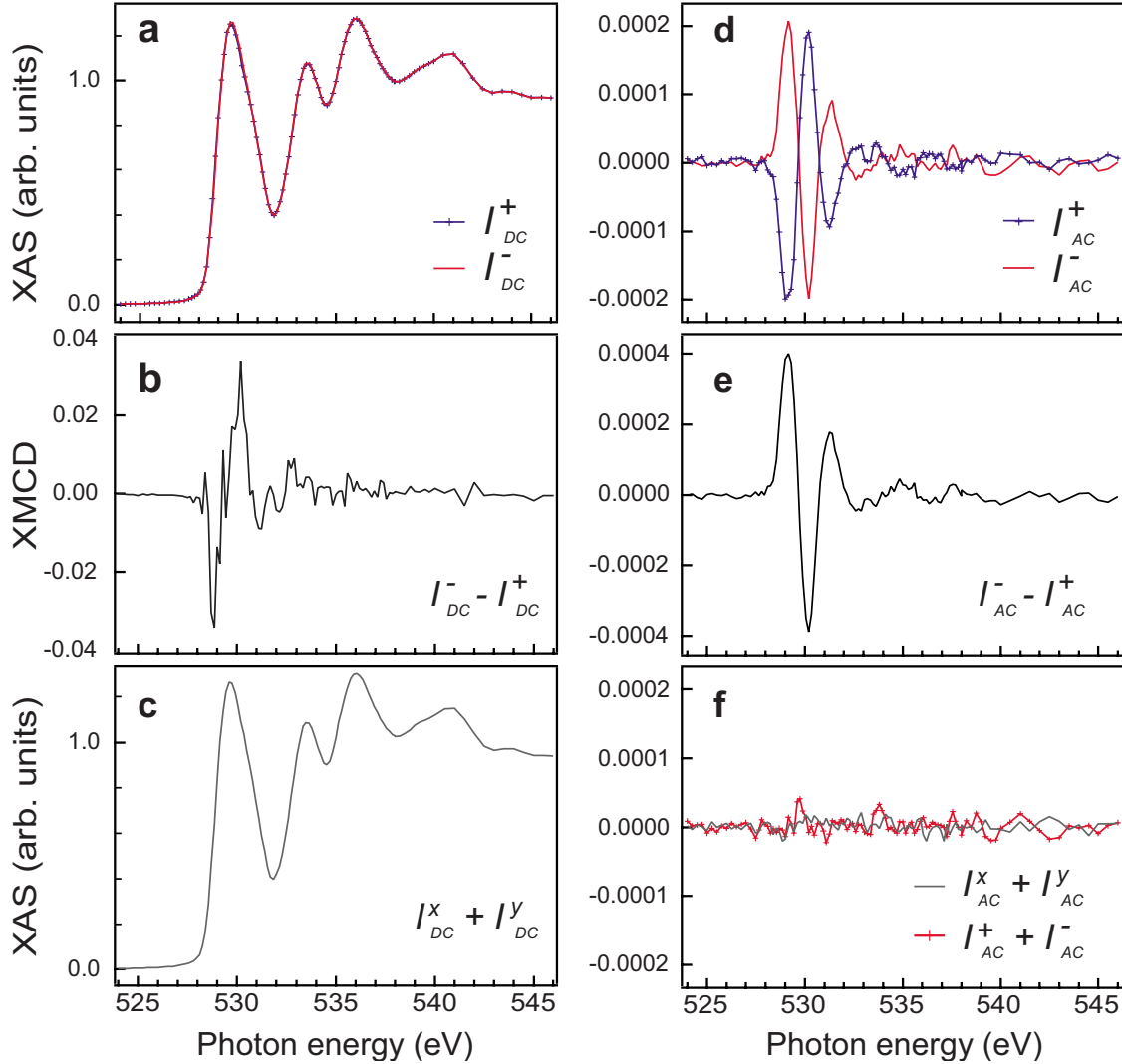
FIG. 3. (Color online) O *K*-edge absorption spectra of YIG. (a) O fluorescence yield as a function of photon energy recorded with positive (I_{dc}^+) and negative (I_{dc}^-) circularly polarized lights. The external field is set to $B_0 = 0.205$ T as in Fig. 2. (b) dc XMCD ($I_{dc}^- - I_{dc}^+$). (c) Linearly polarized dc XAS ($I_{dc}^x + I_{dc}^y$). (d) Double-resonance circularly polarized spectra (I_{ac}^+, I_{ac}^-) recorded simultaneously with (a). (e) Double-resonance XMCD ($I_{ac}^- - I_{ac}^+$) and (f) comparison between the sum of circularly and linearly polarized double-resonance components. For each polarization, a pair of dc and ac spectra was measured in one sweep with a recording time of 1000 s.

Based on these measurements, we suggest that MW absorption at O sites is a general property of magnetic oxides that has eluded detection until now. By knowing precisely the x-ray energy at which the $I_{ac}^\pm$ is nonzero, it is possible to measure the element-resolved FMR spectrum of YIG by sweeping $\mathbf{B}_0$ across the resonance field. Figure 4 shows that the O and Fe traces measured at a fixed photon energy of 530.2 and 708.2 eV, respectively, are clearly superposed to each other, revealing that the O polarization is dynamically coupled to the Fe resonance. Note that the two FMR spectra have the broad asymmetric profile expected under foldover conditions characteristic of the nonlinear regime at high MW power.[30] O atoms thus absorb MW radiation at the same frequency of Fe. As O is the most abundant element in garnets and ferrites, one can argue that O sites shall be included in microscopic models of ferrimagnetic oxides treating dynamic excitations. Further, because of their orbital-magnetization components, O ions are expected to contribute

to spin-orbit-mediated relaxation mechanisms that have so far not been taken into consideration.[25]

B. Double-resonant x-ray microwave absorption in Gd-doped permalloy

Local magnetic-resonance phenomena in metallic films are of great current interest, as they eventually relate to damping,[31] MW emission induced by electron-magnon scattering,[32] as well as MW-assisted magnetization reversal mechanisms.[33] Figure 6 shows the Fe dual-resonance spectra of $Ni_{72}Fe_{18}Gd_{10}$ recorded at the FMR field $B_0 = 0.52$ T. Compared to YIG, we observe much broader Fe $I_{ac}^\pm$ features, which have essentially the same width as the $I_{dc}^\pm$ L_3 and L_2 peaks. This indicates that MW absorption takes place between relatively broad *d*-electron states and that the magnetic sublevels coupled by the MW field are merged into an extended angular momentum-projected DOS. There are several
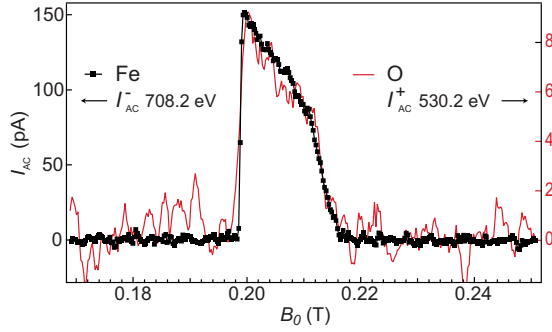
FIG. 4. (Color online) Element-resolved FMR spectra of YIG. Fixed x-ray energy double resonance Fe L_3 and O K-edge intensity recorded as a function of external field B_0. To compare FMR traces with the same sign, Fe (left scale) and O (right scale) spectra of opposite polarization are shown. The spectra are averages of two and four sweeps, each lasting 70 s with lock-in time constants set to 0.1 and 0.2 s, for Fe and O, respectively.

other qualitative spectral differences between Fe species in Permalloy and YIG; notably in Permalloy we find $I_{ac}^+ \approx -I_{ac}^-$ and $I_{ac}^\pm \propto \pm(I_{dc}^- - I_{dc}^+)$, in evident contrast with YIG. These two relationships can be obtained by Eqs. (A1) and (A2) in Appendix by assuming $I^0 = \frac{1}{2}(I^+ + I^-)$, i.e., the equivalency of linearly polarized measurements performed with the **E** vector parallel and perpendicular to the sample magnetization. This is the case when x-ray magnetic linear dichroism (XMLD) effects are small, as in polycrystalline samples and itinerant systems with cubic symmetry, such as Permalloy.[28] We note further that our observations confirm the validity of the widely employed approximation $I^0 \approx \frac{1}{2}(I^+ + I^-)$ in the XMCD sum-rules analysis of itinerant metal systems[34] but raise serious objections to its use in the case of magnetic oxides and strongly correlated compounds. Remarkably, XMLD effects are negligible also for O in YIG where the same equalities between MW spectra hold as for Fe in Permalloy, but for quite a different reason. In the O case, zero XMLD is expected for K-edge transitions due to the spin-only angular momentum of $1s$ core electrons.[28]

C. Comparison between static- and double-resonant XMCD

The ac XMCD intensity measures the change in the magnetic-moment component parallel to $\hat{z}$ (Fig. 1) due to MW absorption. As the precessional motion of the magnetic moments results in a decrease in their longitudinal projection with respect to the equilibrium value, the sign of the ac XMCD is always opposite to the dc signal. This straightforward point had been evidenced by the first FMR measurements performed at fixed x-ray energy[16] (also called XFMR) and finds confirmation in the double-resonance spectra of Figs. 2, 3, and 5. The ratio between ac and dc XMCD intensities can further be analyzed to derive the effective precession angles of the spin and orbital magnetic moments by means of the energy-integrated XMCD sum rules, as discussed in Ref. 17, or by combining L_2- and L_3-edge fixed energy measurements, as argued in Ref. 19. Here, we report the compelling observation that $(I_{ac}^+ - I_{ac}^-) \propto -(I_{dc}^+ - I_{dc}^-)$ independently on the absorption edge and material (Fig. 6). This

relationship is verified to a good degree of approximation at each x-ray photon energy. An important consequence of this equality is that the probability of MW absorption in either a magnetic oxide or metal is proportional to the unperturbed magnetic density of states above the Fermi level probed by conventional dc XMCD, and is therefore homogeneous over the $3d$ states independently of solid-state effects. Small deviations from such behavior are observed, especially in YIG, which may be related to different MW absorption and relaxation rates at T_d and O_h Fe^{3+} sites or to the anisotropy of the crystal field and exchange coupling influencing the electron states available for MW absorption and relaxation.[35] We hope that the present work will stimulate a detailed analysis of such effects, which require combining atomic multiplet theory[10] and MW-induced excitations in XAS simulations.

IV. CONCLUSIONS

In summary, we report double-resonance-spectroscopy experiments involving MW and x-ray absorption. The energy and polarization dependence of core-to-valence x-ray transitions reveals shell-specific electronic excitations driven by MW absorption and related angular momentum transfer. MW transitions are shown to occur homogeneously over the angular momentum-projected DOS, reflecting the hybridization character of the $3d$ bands in metals and insulators. We observe that MW absorption occurs for O as well as Fe atoms in YIG, which leads to the formation of dynamic $2p$-orbital-magnetization components at O sites coupled to the Fe magnetic moments at T_d and O_h sites. Oxygen orbital components may provide a hitherto unknown additional channel for spin-orbit-mediated relaxation in ferrimagnetic oxides. By effectively projecting out a spin-wave state onto specific atomic sites, double-resonant x-ray MW measurements allow us to investigate the perturbed electronic and magnetic configurations of a material in a local way, in addition to the macroscopic magnetization behavior usually probed by FMR.

APPENDIX: ATOMIC MODEL OF DOUBLE-RESONANT X-RAY MICROWAVE ABSORPTION

Even though theoretical efforts to relate electronic perturbations to magnetization dynamics have made substantial progress in recent years,[37–39] an exhaustive treatment of FMR in terms of realistic electron states is not available. Here, we introduce a simplified ionic-like model of double-resonant x-ray MW absorption, which explains some of its most salient spectral features, and enables us to contrast and compare magnetic-resonance results obtained for different elemental species and materials. The simultaneous absorp-
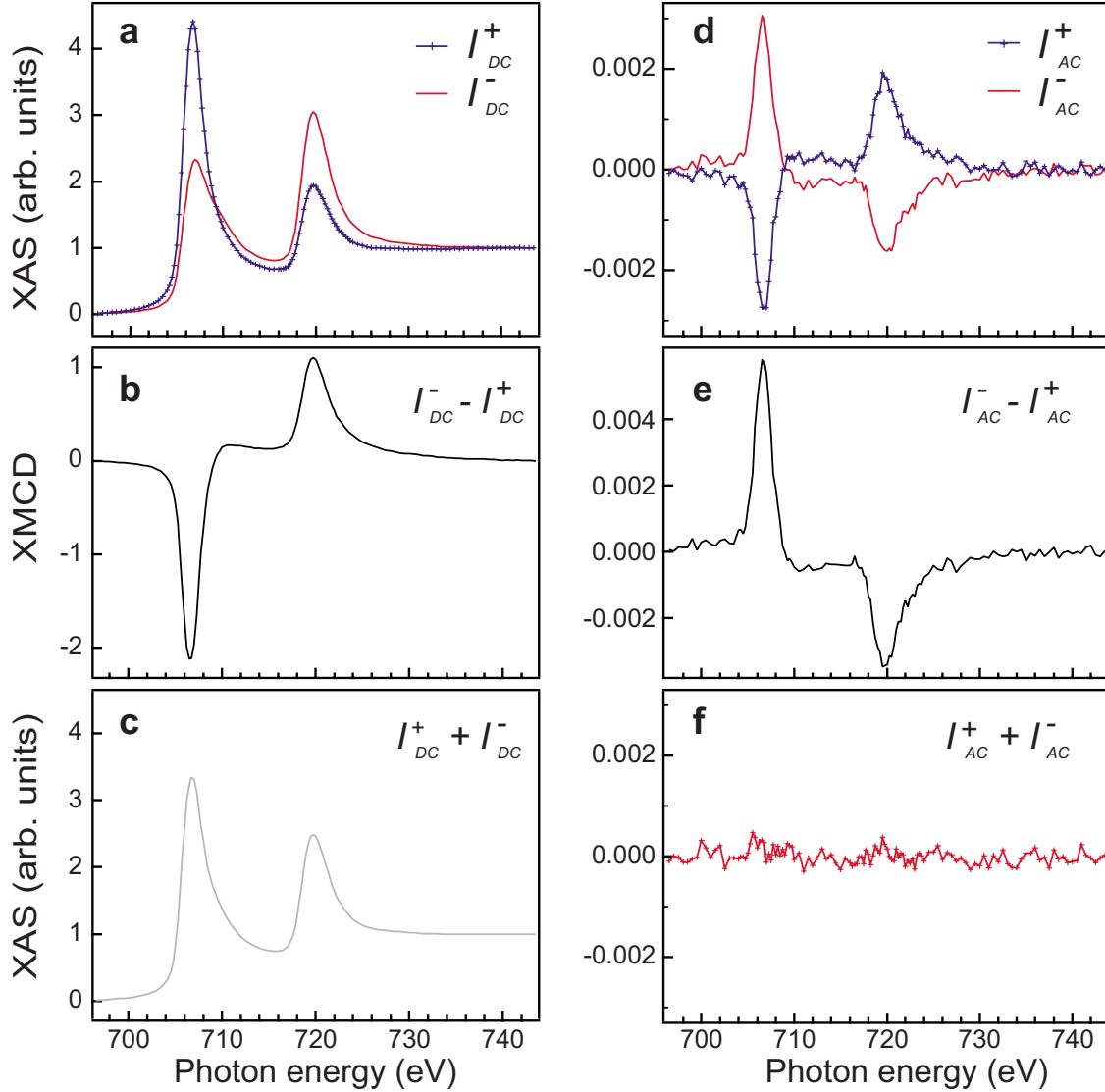
FIG. 5. (Color online) Fe $L_{2,3}$-edge absorption spectra of $Ni_{72}Fe_{18}Gd_{10}$. (a) dc Fe fluorescence yield (I_{dc}^+, I_{dc}^-) as a function of photon energy recorded for circularly polarized light at the resonance field $B_0=0.52$ T. (b) dc XMCD. (c) Sum of dc circularly polarized components. (d) Double-resonance circularly polarized spectra (I_{ac}^+, I_{ac}^-) recorded simultaneously with (a). (e) ac XMCD and (f) sum of circularly-polarized double resonance components.

tion of MW and x-ray photons is schematized in Fig. 7. As appropriate for Fe^{3+}, we consider a $^6S_{5/2}$ ground-state split by a magnetic field into ($2J+1$) Zeeman sublevels $M=-J,...,$ $+J$. For simplicity, among all possible final states, only the $J'=3/2$ multiplet is shown in Fig. 7, where J' is the total (core plus valence shell) angular momentum vector. The XAS spectrum is composed by all dipole-allowed transitions from the ground state to final states having $J'=J, J\pm 1$ with $\Delta M=+1, -1, 0$ corresponding to the I^+, I^-, and I^0 spectral components.

According to Boltzmann statistics, states with lower M are more populated, producing a finite magnetization and giving rise to XMCD.[36,40] Exposure to MW radiation, with consequent absorption of energy, upsets the thermal population of the magnetic sublevels leading to a new equilibrium state where MW absorption is balanced by relaxation to the spin, electronic, and vibrational degrees of freedom of the

material. Therefore, the spectral weight of the different $|JM\rangle \rightarrow |J'M'\rangle$ transitions changes in response to MW absorption, which is the process reflected by the I_{ac} spectra. Moreover, the absorption of energy from the MW field is accompanied by the transfer of angular momentum. A signature of this effect is the different line shape observed for the linearly polarized spectra $I_{ac}^{x,y}$ compared to $I_{dc}^{x,y}$. Coupling of the $|JM\rangle$ levels at resonance induces a coherence between the states which is equivalent to a transverse-magnetization component $\mathbf{M}_\perp$ precessing about $\mathbf{B}_0$ at the internal-field Zeeman splitting frequency. Thus, $I_{ac}^{x,y}$ probes transitions with the electric-field vector $\mathbf{E} \| \mathbf{M}_\perp$, corresponding to $\Delta M=0$ (I^0), while $I_{dc}^{x,y}$ probes $\mathbf{E} \perp \mathbf{M}_z$, i.e., the sum of $\Delta M=\pm 1$ excitations $\frac{1}{2}(I^+ + I^-)$. Such transitions are not equivalent in localized electron systems[36,40] and may give rise to very different absorption spectra, as observed in Fig. 2. Note that, as $\mathbf{M}_\perp$ rotates at 2.25 GHz in the xy plane, I_{ac}^x and I_{ac}^y effectively
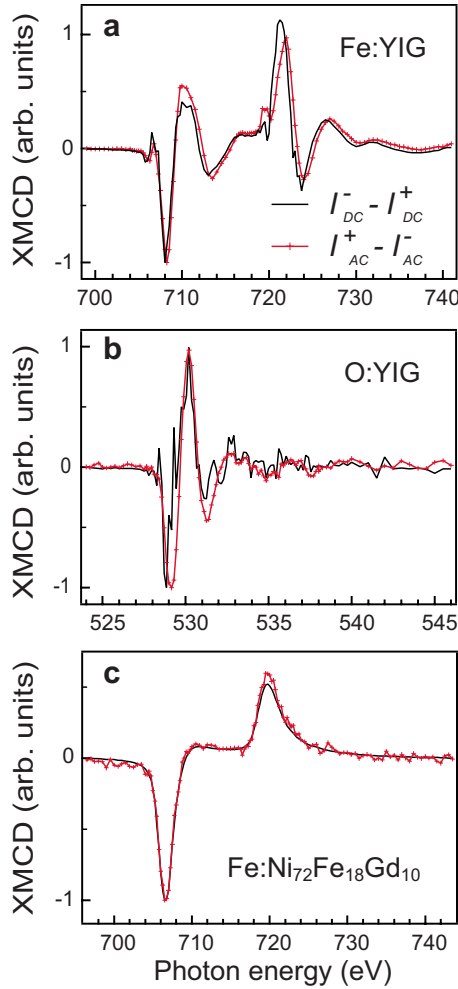
FIG. 6. (Color online) Comparison between the static and double resonance XMCD line shape. (a) Fe and (b) O XMCD spectra of YIG. (c) Fe XMCD of $Ni_{72}Fe_{18}Gd_{10}$. See text for the experimental parameters. To compare the DC and AC intensity, the AC spectra have been multiplied by -1 and scaled to the most intense L_3 (K) edge feature for Fe (O).

depend on the time average of the projection $|\mathbf{E} \cdot \mathbf{M}_\perp|$.

The scheme presented in Fig. 7 is strictly valid only for a free ion or, equivalently, for an electron-paramagnetic-resonance experiment. In such a case, magnetic-resonance transitions occur when the MW frequency matches the Zeeman splitting produced by an external field. In a solid, the magnetic sublevels are split by the internal exchange field, which are orders of magnitude greater compared to typical MW energies. As is well known, however, resonant excitations in ferromagnets and ferrimagnets take place between eigenstates of the total spin Hamiltonian, the energy separation of which is well within the MW range and much smaller than that of one spin-flip event on a single exchange-coupled ion. In other words, MW-induced spin deviations do not remain localized at atomic sites but propagate through the lattice giving rise to a spin wave, namely, a superposition of atomic states with one reduced spin.[41] Despite the collective character of spin waves, however, the localization of core-level transitions makes XAS uniquely sensitive to the charge, spin, and orbital expectation values at the lattice site where
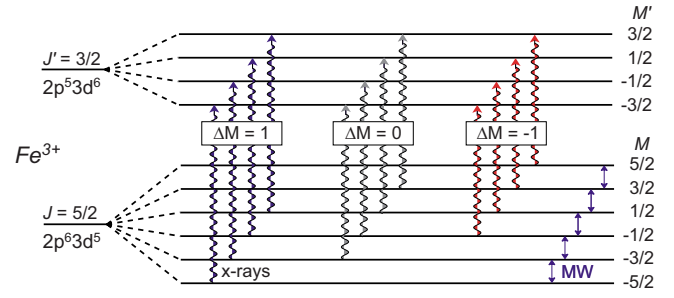

FIG. 7. (Color online) Free-ion model of double-resonance microwave and x-ray excitations for the $^6S_{5/2}$ ground state of Fe^{3+} split by an external field into $(2J+1)$ Zeeman sublevels $M = -J, \ldots, +J$. X-ray-induced transitions to a final state with $J' = \frac{3}{2}$ are shown, where J' is the vector sum of the core $2p$ and valence $3d$ electrons (Ref. 36). MW absorption resonant with the energy difference between Zeeman sublevels modifies the relative x-ray absorption intensity of $|JM\rangle \to |J'M'\rangle$ lines, producing small changes in the x-ray absorption cross section.

the photoexcitation process takes place. These phenomena are critical to reach a microscopic description of magnetic resonance in solids where exchange-coupling and band-structure effects have so far limited investigations to macroscopic observables.

Since the isotropic absorption yield $I^+ + I^- + I^0$ must remain constant[28] and observing that each I_{ac} component effectively measures the *change* in static intensity (δI) due to MW absorption, we can write the following relationships for the absorption intensity:

$$I_{ac}^\pm = -\delta I^\pm + \delta I^0, \tag{A1}$$

$$I_{ac}^{x,y} = -\delta I_{\mathbf{E}\perp\mathbf{M}_z}^{x,y} + \delta I^0 = -\frac{1}{2}(\delta I^+ + \delta I^-) + \delta I^0, \tag{A2}$$

where the first term on the right-hand side of Eq. (A1) represents the decrease in intensity in the $\Delta M = \pm 1$ channel due to the MW-induced depopulation of the lowest magnetic sublevels, and the second term represents the transfer of this intensity to the $\Delta M = 0$ component due to the existence of a transverse-precessing magnetic moment. Note that, by definition,[40] $I^0 = I_{\mathbf{E}\parallel\mathbf{M}_\perp}^{x,y}$. Similar considerations hold for Eq. (A2). Thus, the unusual $I_{ac}^\pm$ spectral shape of Fig. 2 is linked to the mixing of I^0 components in the circularly polarized MW spectra. By taking appropriate linear combinations of Eqs. (A1) and (A2), this model further predicts $(I_{ac}^+ - I_{ac}^-) \propto -(I_{dc}^+ - I_{dc}^-)$ and $I_{ac}^x + I_{ac}^y = I_{ac}^+ + I_{ac}^-$. As the energy dependence of the x-ray absorption intensity is taken into account, the first equality depends on the uniformity of the deviations δI over the entire spectral range while the second is always valid as it expresses the equivalency of circular- and linear-polarization basis states. Equations (A1) and (A2) are indeed quite general as they do not depend on a specific choice of element or absorption edge, and allow us to interpret the main qualitative features of the dual-resonant spectra of both Fe and O in different class of materials such as insulating oxides or metals.

*pietro.gambardella@icrea.es

[1] J. Brossel and F. Bitter, Phys. Rev. **86**, 308 (1952).

[2] H. G. Dehmelt, Phys. Rev. **105**, 1924 (1957).

[3] N. Bloembergen, P. S. Pershan, and L. R. Wilcox, Phys. Rev. **120**, 2014 (1960).

[4] J. Kohler, J. A. J. M. Disselhorst, M. C. J. M. Donckers, E. J. J. Groenen, J. Schmidt, and W. E. Moerner, Nature (London) **363**, 242 (1993).

[5] J. Wrachtrup, C. von Borczyskowski, J. Bernard, M. Orritt, and R. Brown, Nature (London) **363**, 244 (1993).

[6] J. Brossel, S. Geschwind, and A. L. Schawlow, Phys. Rev. Lett. **3**, 548 (1959).

[7] J. Köhler, Phys. Rep. **310**, 261 (1999).

[8] J. J. F. Dillon, H. Kamimura, and J. P. Remeika, J. Appl. Phys. **34**, 1240 (1963).

[9] K. Gnatzig, H. Dötsch, M. Ye, and A. Brockmeyer, J. Appl. Phys. **62**, 4839 (1987).

[10] F. de Groot and A. Kotani, *Core Level Spectroscopy of Solids* (CRC, Boca Raton, 2007).

[11] W. E. Bailey, L. Cheng, D. J. Keavney, C.-C. Kao, E. Vescovo, and D. A. Arena, Phys. Rev. B **70**, 172403 (2004).

[12] A. Puzic *et al.*, J. Appl. Phys. **97**, 10E704 (2005).

[13] D. A. Arena, E. Vescovo, C.-C. Kao, Y. Guan, and W. E. Bailey, Phys. Rev. B **74**, 064409 (2006).

[14] D. A. Arena, E. Vescovo, C.-C. Kao, Y. Guan, and W. E. Bailey, J. Appl. Phys. **101**, 09C109 (2007).

[15] T. Martin, G. Woltersdorf, C. Stamm, H. A. Dürr, R. Mattheis, C. H. Back, and G. Bayreuther, J. Appl. Phys. **103**, 07B112 (2008).

[16] G. Boero, S. Rusponi, P. Bencok, R. S. Popovic, H. Brune, and P. Gambardella, Appl. Phys. Lett. **87**, 152503 (2005).

[17] G. Boero, S. Mouaziz, S. Rusponi, P. Bencok, F. Nolting, S. Stepanow, and P. Gambardella, New J. Phys. **10**, 013011 (2008).

[18] J. Goulon, A. Rogalev, F. Wilhelm, N. Jaouen, C. Goulon-Ginet, G. Goujon, J. B. Youssef, and M. V. Indenbom, JETP Lett. **82**, 696 (2005).

[19] J. Goulon, A. Rogalev, F. Wilhelm, N. Jaouen, C. Goulon-Ginet, and C. Brouder, Eur. Phys. J. B **53**, 169 (2006).

[20] J. Goulon, A. Rogalev, F. Wilhelm, C. Goulon-Ginet, and G. Goujon, J. Synchrotron Radiat. **14**, 257 (2007).

[21] J. Goulon, A. Rogalev, F. Wilhelm, N. Jaouen, C. Goulon-Ginet, G. Goujon, J. B. Youssef, and M. V. Indenbom, J. Electron Spectrosc. Relat. Phenom. **156-158**, 38 (2007).

[22] C. Stamm *et al.*, Nature Mater. **6**, 740 (2007).

[23] A. F. Bartelt, A. Comin, J. Feng, J. R. Nasiatka, T. Einmüller, B. Ludescher, G. Schütz, H. A. Padmore, A. T. Young, and A. Scholl, Appl. Phys. Lett. **90**, 162503 (2007).

[24] P. Rudolf, F. Sette, L. H. Tjeng, G. Meigs, and C. T. Chen, J. Magn. Magn. Mater. **109**, 109 (1992).

[25] A. G. Gurevich and G. A. Melkov, *Magnetization Oscillations and Waves* (CRC, Boca Raton, 1996).

[26] M. Bonnet, A. Delapalme, H. Fuess, and P. Becker, J. Phys. Chem. Solids **40**, 863 (1979).

[27] F. M. F. de Groot, M. Grioni, J. C. Fuggle, J. Ghijsen, G. A. Sawatzky, and H. Petersen, Phys. Rev. B **40**, 5715 (1989).

[28] J. Stöhr and H. C. Siegmann, *Magnetism: From Fundamentals to Nanoscale Dynamics* (Springer, Berlin, 2006).

[29] J.-i. Igarashi and K. Hirai, Phys. Rev. B **50**, 17820 (1994).

[30] Y. T. Zhang, C. E. Patton, and G. Srinivasan, J. Appl. Phys. **63**, 5433 (1988).

[31] S. G. Reidy, L. Cheng, and W. E. Bailey, Appl. Phys. Lett. **82**, 1254 (2003).

[32] L. Berger, Phys. Rev. B **54**, 9353 (1996).

[33] G. Woltersdorf and C. H. Back, Phys. Rev. Lett. **99**, 227207 (2007).

[34] C. T. Chen, Y. U. Idzerda, H.-J. Lin, N. V. Smith, G. Meigs, E. Chaban, G. H. Ho, E. Pellegrin, and F. Sette, Phys. Rev. Lett. **75**, 152 (1995).

[35] K. A. Wickersheim and R. L. White, Phys. Rev. Lett. **8**, 483 (1962).

[36] G. van der Laan and B. T. Thole, Phys. Rev. B **42**, 6670 (1990).

[37] J. Kuneš and V. Kamberský, Phys. Rev. B **65**, 212411 (2002).

[38] D. Steiauf and M. Fähnle, Phys. Rev. B **72**, 064450 (2005).

[39] K. Gilmore, Y. U. Idzerda, and M. D. Stiles, J. Appl. Phys. **103**, 07D303 (2008).

[40] B. T. Thole, G. van der Laan, and G. A. Sawatzky, Phys. Rev. Lett. **55**, 2086 (1985).

[41] J. Van Kranendonk and J. H. Van Vleck, Rev. Mod. Phys. **30**, 1 (1958).